

The Nature of the Transition Metal–Carbonyl Bond and the Question about the Valence Orbitals of Transition Metals. A Bond-Energy Decomposition Analysis of $\text{TM}(\text{CO})_6^q$ ($\text{TM}^q = \text{Hf}^{2-}, \text{Ta}^-, \text{W}, \text{Re}^+, \text{Os}^{2+}, \text{Ir}^{3+}$)[†]

Axel Diefenbach,[‡] F. Matthias Bickelhaupt,^{§,*} and Gernot Frenking^{‡,*}

Contribution from the Fachbereich Chemie, Philipps-Universität Marburg, Hans-Meerwein-Strasse, D-35032 Marburg, Germany and the Scheikundig Laboratorium der Vrije Universiteit, De Boelelaan 1083, NL-1081 HV Amsterdam, The Netherlands

Received February 23, 2000. Revised Manuscript Received May 9, 2000

Abstract: The equilibrium geometries and bond-dissociation energies for loss of one CO and loss of six CO from $\text{TM}(\text{CO})_6^q$ ($\text{TM}^q = \text{Hf}^{2-}, \text{Ta}^-, \text{W}, \text{Re}^+, \text{Os}^{2+}, \text{Ir}^{3+}$) have been calculated at the BP86 level using Slater type basis sets. The bonding interactions between $\text{TM}(\text{CO})_5$ and one CO and between TM^q in the t_{2g}^6 valence state and the ligand cage $(\text{CO})_6$ were analyzed in the framework of Kohn-Sham MO theory with the use of the quantitative ETS energy-partitioning scheme. The BDEs exhibit a U-shaped curve from $\text{Hf}(\text{CO})_6^{2-}$ to $\text{Ir}(\text{CO})_6^{3+}$, with $\text{W}(\text{CO})_6$ having the lowest BDE for loss of one CO while $\text{Re}(\text{CO})_6^+$ has the lowest BDE for loss of 6 CO. The stabilizing orbital interaction term, ΔE_{orb} , and the electrostatic attraction term, ΔE_{elstat} , have comparable contributions to the $(\text{CO})_5\text{TM}^q\text{--CO}$ bond strength. The largest orbital contributions relative to the electrostatic attraction are found for the highest charged complexes, $\text{Hf}(\text{CO})_6^{2-}$ and $\text{Ir}(\text{CO})_6^{3+}$. The contribution of the $(\text{CO})_5\text{TM}^q\text{--CO}$ σ donation continuously increases from $\text{Hf}(\text{CO})_6^{2-}$ to $\text{Ir}(\text{CO})_6^{3+}$ and eventually becomes the dominant orbital interaction term in the carbonyl cations, while the $(\text{CO})_5\text{TM}^q\text{--CO}$ π -back-donation decreases in the same direction. The breakdown of the contributions of the d, s, and p valence orbitals of the metals to the energy and charge terms of the $\text{TM}^q\text{--}(\text{CO})_6$ donation shows for a single AO the order $d \gg s > p$, but the contributions of the three p orbitals of TM^q are larger than the contribution of the s orbital.

Introduction

The nature of the chemical bond is at the very heart of chemical research. The lack of true insight into the interatomic interactions in molecules in the prequantum chemical period prior to 1925¹ forced chemists to use heuristic models that were developed by correlating experimental observations with plausible ad-hoc assumptions. Whereas these models proved to be very helpful as an ordering scheme for experimental observations and as a tool for the design of new experiments, they do not provide any information about the nature of the chemical bond. Only after sophisticated quantum chemical methods were developed and powerful computers were available did it become possible to accurately analyze the interatomic interactions of molecules and to understand the physical nature of the chemical bond. The progress in quantum chemistry also contributed to the development of bonding models, with molecular orbital (MO) theory being the most prominent example. MO theoretical models belong now to the standard curriculum of modern chemical textbooks.

The enormous success of MO theory, particularly in form of the frontier molecular orbital model,² led to its widespread use

in organic and inorganic chemistry for explaining the structure and reactivity of molecules. There is a danger, however, in the uncritical use of the frontier orbital model for explaining chemical bonding, because other factors such as electrostatic interactions and Pauli repulsion may also play a significant role. A thorough analysis of the different factors which contribute to the strength of the interatomic interactions is seldom done, and the results of such studies often reveal that the nature of the chemical bond is more complicated than the simple bonding models which are commonly used. Nevertheless, it is fair to say that much progress has been made in the understanding of the chemical bond in the past decades.

Most quantum chemical analyses of the chemical bond focused, in the beginning, on the elements of the first row of the periodic system. The extension of the bonding concepts which were developed for the first octal row to the heavier main-group elements already has proven to be more complicated than most chemists would have expected.³ Nevertheless, quantum chemical calculations gave insight into the bonding situation of the main-group elements beyond neon. A detailed analysis of the multiple bonds of light and heavy main-group elements, which led to some surprising results, gave an understanding for the different geometries and significantly lower stabilities of molecules with multiple bonds between heavier elements.^{3,4} The

[†] Theoretical Studies of Organometallic Compounds. Part 42. Party 41: Deubel, D.; Sundermeyer, J.; Frenking, G. *J. Am. Chem. Soc.*, submitted for publication.

[‡] Philipps-Universität Marburg.

[§] Vrije Universiteit Amsterdam.

(1) Heitler, W.; London, F. *Z. Physik*, **1927**, *44*, 455.

(2) (a) Fukui, K. *Acc. Chem. Res.* **1971**, *4*, 57. (b) Fleming, I. *Frontier Orbitals and Organic Chemical Reactions*; Wiley: New York, 1976.

(3) Kutzelnigg, W. *Angew. Chem.* **1984**, *96*, 262; *Angew. Chem., Int. Ed. Engl.* **1984**, *23*, 272.

(4) (a) Schmidt, M. W.; Truong, P. N.; Gordon, M. S. *J. Am. Chem. Soc.* **1987**, *109*, 5217. (b) Jacobsen, H.; Ziegler, T. *J. Am. Chem. Soc.* **1994**, *116*, 3667.

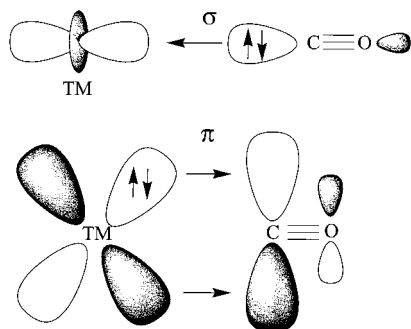


Figure 1. Schematic representation of the TM–CO orbital interactions in carbonyl complexes. TM←CO σ -donation (top) and TM→CO π -back-donation (bottom).

long-lasting controversy about the question of whether the d orbitals of the heavier main group elements should be considered as true valence orbitals was finally solved with the help of sophisticated methods for analyzing the electronic structure in favor of the sp -valence-bonding model.⁵

Theoretical analyses of the chemical bond of transition-metal (TM) compounds which are based on accurate quantum chemical calculations could only be made in the more recent past, because the electronic structure of the TMs is more complex. Previous studies based on approximate MO methods, particularly by Hoffmann, demonstrated that MO arguments are very helpful in explaining the structures and geometries of TM compounds.⁶ However, two detailed analyses of the Cr–CO interactions in Cr(CO)₆ by Davidson et al.^{7a} and by Baerends and Rozendaal^{7b} have shown that the nature of the chemical bond in chromium hexacarbonyl is much more complicated than it may be assumed by considering qualitative models such as the popular Dewar–Chatt–Duncanson (DCD) model⁸ of TM←CO σ -donation and TM→CO π -back-donation (Figure 1).

Inspection of the different energy terms for the metal–ligand interactions which were identified with the Morokuma energy-partitioning scheme⁹ showed that the contribution of the Cr→CO π -back-donation to the total binding energy is larger than the energy term which comes from the Cr←CO σ -donation. This is in agreement with numerous earlier theoretical studies of metal–CO interactions.¹⁰ However, analysis of the changes in the electronic structure by Davidson et al.⁷ revealed that the driving force for the large π -back-bonding is the electrostatic energy that arises from the penetration of the 5 σ electrons, which are the carbon-lone-pair electrons, into the chromium valence shell. The authors pointed out that electrostatic forces and the Pauli exclusion principle must be considered for a true understanding of the chemical bonding.

(5) (a) Reed, A.; Schleyer, P. v. R. *J. Am. Chem. Soc.* **1990**, *112*, 1434. (b) Magnusson, E. *J. Am. Chem. Soc.* **1990**, *112*, 7940. (c) Cioslowski, J.; Mixon, S. T. *Inorg. Chem.* **1993**, *32*, 3209. (d) Cooper, D. L.; Cunningham, T. P.; Gerratt, J.; Karadakov, P. B.; Raimondi, M. *J. Am. Chem. Soc.* **1994**, *116*, 4414. (e) Häser, M. *J. Am. Chem. Soc.* **1996**, *118*, 7311. (f) Dobado, J. A.; Martinez-Garcia, H.; Molina, J. M.; Sundberg, M. R. *J. Am. Chem. Soc.* **1998**, *120*, 8461.

(6) (a) Hoffmann, R.; Chen, M. M. L.; Thorn, D. L. *Inorg. Chem.* **1977**, *16*, 503. (b) Schilling, B. E. R.; Hoffmann, R. *J. Am. Chem. Soc.* **1979**, *101*, 3456. (c) Hoffmann, R. *Science (Washington, D.C.)* **1981**, *211*, 995. (d) Hoffmann, R.; Albright, T. A.; Thorn, D. L. *Pure Appl. Chem.* **1978**, *50*, 1. (e) Jean, Y.; Lledos, A.; Burdett, J. K.; Hoffmann, R. *J. Am. Chem. Soc.* **1988**, *110*, 4506, and further references cited therein.

(7) (a) Davidson, E. R.; Kunze, K. L.; Machado, F. B. C.; Chakravorty, S. J. *Acc. Chem. Res.* **1993**, *26*, 628. (b) Baerends, E. J.; Rozendaal, A. In *Quantum Chemistry: The Challenge of Transition Metals and Coordination Chemistry*; Proceedings of the NATO ASI; Veillard, A., Ed; Reidel: Dordrecht, Germany, 1986; p 159.

(8) (a) Dewar, M. J. S. *Bull. Soc. Chim. Fr.* **1951**, *18*, C79. (b) Chatt, J.; Duncanson, L. A. *J. Chem. Soc.* **1953**, 2929.

(9) Morokuma, K. *Acc. Chem. Res.* **1977**, *10*, 294.

It is possible to maintain the conceptual power of the MO model and at the same time consider all energy components including correlation energy for the chemical bonding by using density functional theory (DFT). Davidson has already shown that the Morokuma energy partitioning of Cr(CO)₆ using Kohn–Sham (KS) orbitals leads to very similar results about the relative size of the Cr→CO π -back-donation and the Cr←CO σ -donation.⁷ A closely related energy decomposition method, the Morokuma analysis,⁹ has been introduced for DFT methods by Ziegler and Rauk.¹¹ It is called extended transition state (ETS) method, and it has been used for analyzing the binding interactions in numerous TM compounds.^{12,13} Details of the method are shortly described in the Methods section.

Most previous theoretical studies which analyzed the chemical bond in TM carbonyls focused on *neutral* complexes. However, TM carbonyls can also be negatively or positively charged. TM carbonyl complexes which carry a positive charge have been intensively investigated in recent years, both experimentally¹⁴ and theoretically.^{15,16} The finding that some complexes, TM-(CO)_{*n*}^{*m+*}, may have C–O stretching frequencies which are higher than those in free CO (2143 cm⁻¹) led Strauss to suggest that they should be called “nonclassical” carbonyls, while carbonyl complexes with $\nu(\text{CO}) < 2143 \text{ cm}^{-1}$ are “classical”.¹⁷ A recent theoretical investigation by Szilagyí and Frenking

(10) (a) Bauschlicher, C. W.; Bagus, P. S. *J. Chem. Phys.* **1984**, *81*, 5889. (b) Bauschlicher, C. W.; Petterson, L. G. M.; Siegbahn, P. E. M. *J. Chem. Phys.* **1987**, *87*, 2129. (c) Bauschlicher, C. W.; Langhoff, S. R.; Barnes, L. A. *Chem. Phys.* **1989**, *129*, 431. (d) Bauschlicher, C. W. *J. Chem. Phys.* **1986**, *84*, 260. (e) Bauschlicher, C. W.; Bagus, P. S.; Nelin, C. J.; Roos, B. O. *Chem. Phys.* **1986**, *85*, 354. (f) Barnes, L. A.; Rosi, M.; Bauschlicher, C. W. *J. Chem. Phys.* **1991**, *94*, 2031. (g) Barnes, L. A.; Rosi, M.; Bauschlicher, C. W. *J. Chem. Phys.* **1990**, *93*, 609. (h) Barnes, L. A.; Bauschlicher, C. W. *J. Chem. Phys.* **1989**, *91*, 314. (i) Blomberg, M. R. A.; Brandemark, U. B.; Siegbahn, P. E. M.; Wennerberg, J.; Bauschlicher, C. W. *J. Am. Chem. Soc.* **1988**, *110*, 6650. (j) Hall, M. B.; Fenske, R. F. *Inorg. Chem.* **1972**, *11*, 1620. (k) Sherwood, P. E.; Hall, M. B. *Inorg. Chem.* **1979**, *18*, 2325. (l) Sherwood, P. E.; Hall, M. B. *Inorg. Chem.* **1980**, *19*, 1805. (m) Williamson, R. L.; Hall, M. B. *Int. J. Quantum Chem.* **1987**, *21S*, 503. (n) Hillier, I. H.; Saunders, V. R. *Mol. Phys.* **1971**, *23*, 1025. (o) Hillier, I. H.; Saunders, V. R. *J. Chem. Soc., Chem. Commun.* **1971**, 642. (p) Ford, P. C.; Hillier, I. H. *J. Chem. Phys.* **1984**, *80*, 5664. (q) Ford, P. C.; Hillier, I. H.; Pope, S. A.; Guest, M. F. *Chem. Phys. Lett.* **1983**, *102*, 555. (r) Cooper, G.; Green, J. C.; Payne, M. P.; Dobson, B. R.; Hillier, I. H. *Chem. Phys. Lett.* **1986**, *125*, 97. (s) Cooper, G.; Green, J. C.; Payne, M. P.; Dobson, B. R.; Hillier, I. H.; Vincent, M.; Rosi, M. *J. Chem. Soc., Chem. Commun.* **1986**, 438. (t) Moncrieff, D.; Ford, P. C.; Hillier, I. H.; Saunders, V. R. *J. Chem. Soc., Chem. Commun.* **1983**, 1108. (u) Smith, S.; Hillier, I. H.; von Niessen, W.; Guest, M. C. *Chem. Phys.* **1989**, *135*, 357. (v) Vanquickenborne, L. G.; Verhulst, J. *J. Am. Chem. Soc.* **1987**, *109*, 4825. (w) Pierfoot, K.; Verhulst, J.; Verbeke, P.; Vanquickenborne, L. G. *Inorg. Chem.* **1989**, *28*, 3059. (x) Yamamoto, S.; Kashiwagi, H. *Chem. Phys. Lett.* **1993**, *205*, 306. (y) Blomberg, M. R. A.; Siegbahn, P. E. M.; Lee, T. L.; Rendell, A. P.; Rice, J. E. *J. Chem. Phys.* **1991**, *95*, 5898.

(11) (a) Ziegler, T.; Rauk, A. *Theor. Chim. Acta* **1977**, *46*, 1. (b) Ziegler, T.; Rauk, A. *Inorg. Chem.* **1979**, *18*, 1558. (c) Ziegler, T.; Rauk, A. *Inorg. Chem.* **1979**, *18*, 1755.

(12) Ehlers, A. W.; Ruiz-Molares, Y.; Baerends, E. J.; Ziegler, T. *Inorg. Chem.* **1997**, *36*, 5031.

(13) Selected examples: (a) Jacobsen, H.; Ziegler, T. *Organometallics* **1995**, *14*, 224. (b) Jacobsen, H.; Ziegler, T. *Inorg. Chem.* **1996**, *35*, 775. (c) Li, J.; Schreckenbach, G.; Ziegler, T. *J. Am. Chem. Soc.* **1995**, *117*, 486. (d) Ehlers, A. W.; Baerends, E. J.; Bickelhaupt, F. M.; Radius, U. *Chem. —Eur. J.* **1998**, *4*, 210.

(14) (a) Strauss, S. H. *Chemtracts* **1997**, *10*, 77. (b) Willner, H.; Aubke, F. *Angew. Chem.* **1997**, *109*, 2506. *Angew. Chem., Int. Ed. Engl.* **1997**, *2402*.

(15) (a) Mavridis, A.; Harrison, J. F.; Allison, J. *J. Am. Chem. Soc.* **1989**, *111*, 2482. (b) Allison, J.; Mavridis, A.; Harrison, J. F. *Polyhedron* **1988**, *7*, 1559. (c) Barnes, L. A.; Rosi, M.; Bauschlicher, C. W. *J. Chem. Phys.* **1990**, *93*, 609. (d) Bauschlicher, C. W.; Barnes, L. A. *Chem. Phys.* **1988**, *124*, 383. (e) Büker, H. J.; Maitre, P.; Ohanessian, G. *J. Phys. Chem. A* **1997**, *101*, 3966. (f) Lupinetti, A. J.; Jonas, V.; Thiel, W.; Strauss, S. H.; Frenking, G. *Chem. Eur. J.* **1999**, *5*, 2573. (g) Veldkamp, A.; Frenking, G. *Organometallics* **1993**, *12*, 4613. (h) Lupinetti, A. J.; Fau, S.; Frenking, G.; Strauss, S. H. *J. Phys. Chem. A* **1997**, *101*, 9551.

(16) Szilagyí, R. K.; Frenking, G. *Organometallics* **1997**, *16*, 4807.

(SF)¹⁶ of the structure and bonding of the isoelectronic hexacarbonyls $\text{TM}(\text{CO})_6^q$ ($\text{TM}^q = \text{Hf}^{2-}, \text{Ta}^-, \text{W}, \text{Re}^+, \text{Os}^{2+}, \text{Ir}^{3+}$) using the charge decomposition analysis (CDA)¹⁸ showed that the $\text{TM}^q \rightarrow \text{CO}$ π -back-donation continuously decreases from Hf^{2-} to Ir^{3+} , which explains why the C–O stretching frequency increases in the same order in intervals of $\sim 100 \text{ cm}^{-1}$.

A surprising result was found for the trend of the first CO bond dissociation energies (BDE) of the hexacarbonyls, which show a U-shaped curve from Hf^{2-} to Ir^{3+} . The lowest BDE was calculated for $\text{W}(\text{CO})_6$. The bond energy increases slightly for $\text{Ta}(\text{CO})_6^-$ and then for $\text{Hf}(\text{CO})_6^{2-}$, and an even stronger increase in the BDE was calculated for the carbonyl cations. $\text{Ir}(\text{CO})_6^{3+}$ clearly has the highest BDE of the six isoelectronic species.¹⁶ This is surprising in light of the results for neutral TM carbonyls, which all agree that the $\text{TM} \rightarrow \text{CO}$ π -back-donation contributes more to the metal–CO bond energy than $\text{TM} \leftarrow \text{CO}$ σ -donation.^{7,10} A plausible explanation would be that either σ -donation becomes much more important in TM carbonyl cations or that electrostatic interactions play a larger role in positively charged species. The higher BDE of the negatively charged carbonyls than that of $\text{W}(\text{CO})_6$ might then be due to larger π -back-donation. Because the molecular charge changes from -2 to $+3$, it might be expected that electrostatic forces significantly influence the strength of the metal–carbonyl interactions.

The question about the change in the size of the energy contributions to the metal–CO interactions when the carbonyl complex is negatively or positively charged was one reason for carrying out this study. Which factors determine the U-shaped trend of the BDE in the metal hexacarbonyls? A second question which we want to address concerns a more fundamental aspect of TM bonding. There is, at present, a controversy about the question of whether the lowest lying empty p orbitals of the transition metals should be considered as valence orbitals or if they are only polarization functions, like the d functions of the main-group elements.^{19,20} The common picture of TM –ligand orbital interactions in an octahedral complex, TML_6 , where the ligands L have σ donor and π acceptor orbitals suggests that $\text{TM} \leftarrow \text{L}$ σ -donation involves the empty d(σ), p, and s orbitals of the metal (Figure 2). A CDA analysis of $\text{W}(\text{CO})_6$ has shown that the $\text{W} \leftarrow \text{CO}$ σ -donation involves mainly the d orbitals, while the s and p orbitals are less important.¹⁸ But how important are the s and p orbitals energetically, and how do the contributions to the bond energy change when the hexacarbonyl complex carries a positive charge? In the course of this work we found that the analysis of the interactions between the metal, TM^q , and the ligand cage, $(\text{CO})_6$, is an excellent probe to address this question. To answer the two questions, we carried out a quantitative bonding analysis of the title compounds in the framework of the Kohn–Sham MO model. This was done with the help of an energy decomposition analysis at the gradient-corrected DFT level using the ETS method. Details are described in the Methods section.

The bonding analysis was carried out in two ways. One way was to look at the interactions between one CO and the $\text{TM}(\text{CO})_5^q$ fragment. The results give insight into the factors which determine the first BDE. In the second approach we analyzed

the interactions between the bare transition metal TM^q and the cage of $(\text{CO})_6$ in octahedral symmetry. This is the approach that has been used by Davidson for his bonding analysis of $\text{Cr}(\text{CO})_6$.⁷ Because O_h symmetry is retained in the latter analysis, it is possible to identify the energy contributions of the d, s, and p orbitals of the metal to the $\text{TM}^q \leftarrow \text{CO}$ σ -donation. An energy analysis of the metal–carbonyl bonding in neutral and charged complexes has recently been reported by Ehlers et al.¹² The authors investigated only the σ - and π -orbital contributions to the first BDE and not the energy components which are due to Pauli repulsion and electrostatic interaction. The bonding between the metal and the ligand cage, $(\text{CO})_6$, and the contributions by the d, s, and p orbitals of the metal were not studied.

Methods

The calculations have been performed at the nonlocal DFT level of theory using the exchange functional of Becke²¹ and the correlation functional of Perdew²² (BP86). Relativistic effects have been considered by the zero-order regular approximation (ZORA),²³ which is more reliable than the widely used Pauli formalism. Uncontracted Slater type orbitals (STOs) have been used as basis functions for the SCF calculations.²⁴ The basis sets for all atoms have triple- ζ quality, augmented with a 6p function on the metal atoms and two sets of polarization functions, 3d and 4f, for carbon and oxygen. The $(1s)^2$ core electrons of oxygen and carbon and the $(1s2s2p3s3p3d4s4p4d)^{46}$ core electrons of the metals were treated by the frozen-core approximation.²⁵ An auxiliary set of s, p, d, f, and g STOs was used to fit the molecular densities and to represent the Coulomb and exchange potentials accurately in each SCF cycle.²⁶ The optimized structures have been verified as minima on the potential energy surface by calculation of the vibrational frequencies. The atomic partial charges have been calculated with the Hirshfeld partitioning scheme.²⁷ All calculations were carried out with the program package ADF.²⁸

The bonding interactions between the pentacarbonyl fragments, $\text{TM}(\text{CO})_5^q$ and CO, and between the metal atom, TM^q , and the ligand cage, $(\text{CO})_6$, have been analyzed with the energy decomposition scheme ETS developed by Ziegler and Rauk.¹¹ Within this method, the bond dissociation energy ΔE between two fragments A and B is partitioned into several contributions which can be identified as physically meaningful entities. First, ΔE is separated into two major components ΔE_{prep} and ΔE_{int} :

$$\Delta E = \Delta E_{\text{prep}} + \Delta E_{\text{int}}$$

ΔE_{prep} is the energy which is necessary to promote the fragments A and B from their equilibrium geometry and electronic ground state to the geometry and electronic state which they have in the compound AB. ΔE_{int} is the instantaneous interaction energy between the two fragments in the molecule. The latter quantity will be the focus of the present work. The interaction energy, ΔE_{int} , can be divided into three

(17) Lupinetti, A. J.; Frenking, G.; Strauss, S. H. *Angew. Chem.* **1998**, *110*, 2229; *Angew. Chem., Int. Ed. Engl.* **1998**, *37*, 2113.

(18) Dapprich, S.; Frenking, G. *J. Phys. Chem.* **1995**, *99*, 9352.

(19) (a) Landis, C. R.; Cleveland, T.; Firman, T. K. *J. Am. Chem. Soc.* **1995**, *117*, 1859. (b) Landis, C. R.; Firman, T. K.; Root, D. M.; Cleveland, T. *J. Am. Chem. Soc.* **1998**, *120*, 1842. (c) Landis, C. R.; Cleveland, T.; Firman, T. K. *J. Am. Chem. Soc.* **1998**, *120*, 2641. (d) Firman, T. K.; Landis, C. R. *J. Am. Chem. Soc.* **1998**, *120*, 12650.

(20) Bayse, C. A.; Hall, M. B. *J. Am. Chem. Soc.* **1999**, *121*, 1348.

(21) Becke, A. D. *Phys. Rev. A: At., Mol., Opt. Phys.* **1988**, *38*, 3098.

(22) Perdew, J. P. *Phys. Rev. B: Condens. Mater.* **1986**, *33*, 8822.

(23) (a) Chang, C.; Pelissier, M.; Durand, Ph. *Phys. Scr.* **1986**, *34*, 394.

(b) Heully, J.-L.; Lindgren, I.; Lindroth, E.; Lundquist, S.; Martensson-Pendrill, A.-M. *J. Phys. B: At. Mol. Opt. Phys.* **1986**, *19*, 2799. (c) van Lenthe, E.; Baerends, E. J.; Snijders, J. G. *J. Chem. Phys.* **1993**, *99*, 4597. (d) van Lenthe, E.; Baerends, E. J.; Snijders, J. G. *J. Chem. Phys.* **1996**, *105*, 6505. (e) van Lenthe, E.; van Leeuwen, R.; Baerends, E. J.; Snijders, J. G. *Int. J. Quantum Chem.* **1996**, *57*, 281.

(24) Snijders, J. G.; Baerends, E. J.; Vernooijs, P. *At. Data Nucl. Data Tables* **1982**, *26*, 483.

(25) Baerends, E. J.; Ellis, D. E.; Ros, P. *Chem. Phys.* **1973**, *2*, 41.

(26) Krijn, J.; Baerends, E. J. *Fit Functions in the HFS-Method*; Internal Report (in dutch); Vrije Universiteit Amsterdam: The Netherlands, 1984.

(27) Hirshfeld, E. L. *Theor. Chim. Acta* **1977**, *44*, 129.

(28) (a) Fonseca Guerra, C.; Snijders, J. G.; te Velde, G.; Baerends, E. *J. Theor. Chem. Acc.* **1998**, *99*, 391. (b) Bickelhaupt, F. M.; Baerends, E. *J. Rev. Comput. Chem.*, Vol. 15, in print.

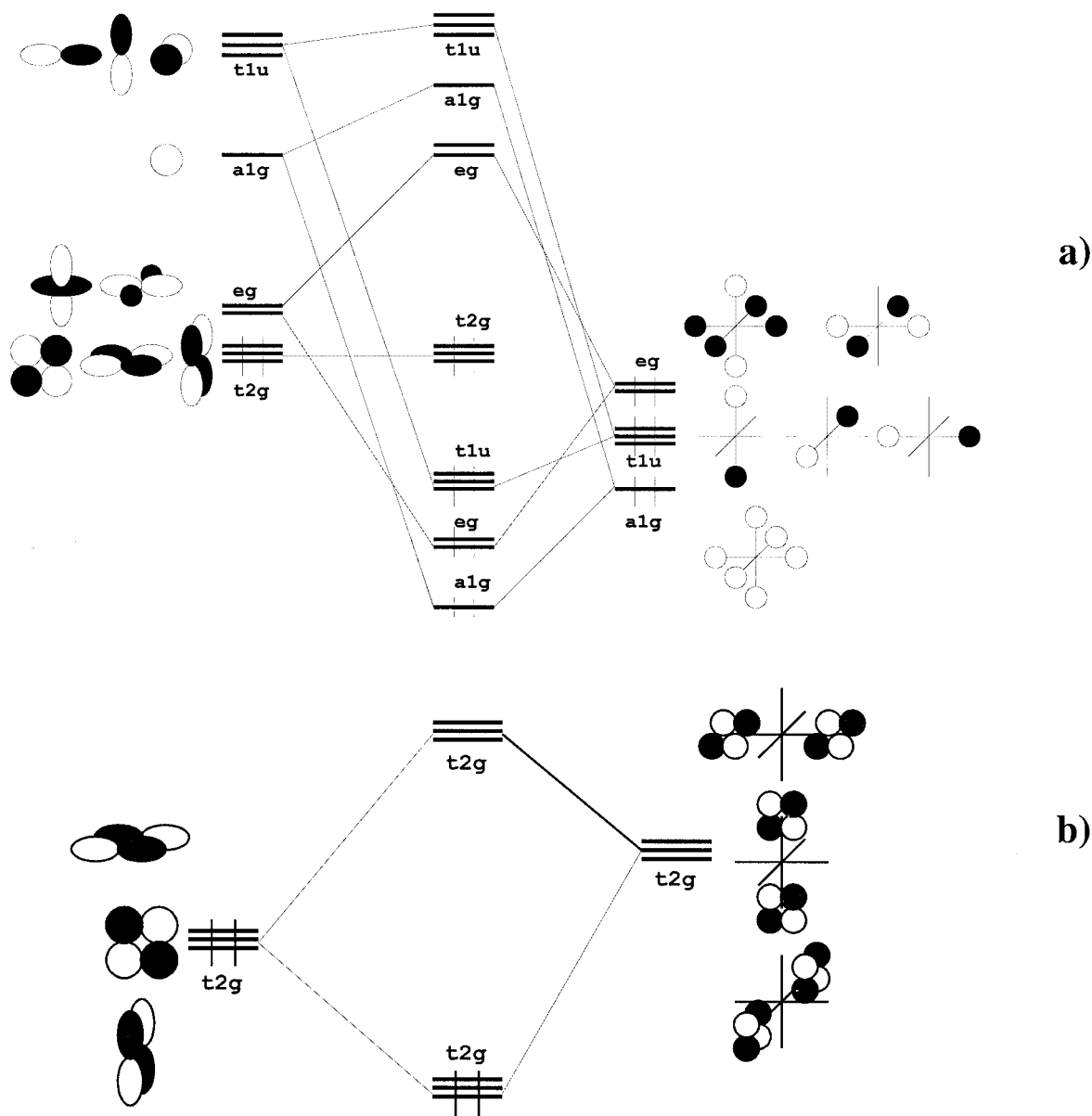


Figure 2. Orbital interaction diagram of the splitting of the d, s, p valence orbitals of a transition metal in an octahedral ligand field. (a) Interactions of the σ orbitals. (b) Interactions of the π orbitals.

main components:^{28b,29}

$$\Delta E_{\text{int}} = \Delta E_{\text{elstat}} + \Delta E_{\text{Pauli}} + \Delta E_{\text{orb}}$$

ΔE_{elstat} gives the electrostatic interaction energy between the fragments which is calculated with a frozen electron density distribution

(29) It has become customary to add the values of ΔE_{Pauli} and ΔE_{elstat} into a common term ΔE° (which is sometimes called the steric term).^{12,13} The bonding analysis is then often carried out in terms of the ΔE° and ΔE_{orb} values, which give a bonding model where the attractive orbital interaction term ΔE_{orb} , and the ΔE° term are compared with the total interaction energy ΔE_{int} . Such a partitioning of the bonding energy often supports the common MO bonding model where the dominant contributions to the chemical bond arise from the interactions between particular orbitals such as the HOMO and LUMO.² However, the addition of ΔE_{Pauli} and ΔE_{elstat} into a single term, ΔE° , is arbitrary and deceptive, because the contribution of the electrostatic forces to the bonding interactions is not obvious anymore. We decided to discuss the values for the three contributions, ΔE_{Pauli} , ΔE_{elstat} and ΔE_{orb} , to the bond energy separately and to compare the trend of the three terms with the net bonding energies. This leads to an unbiased conclusion about the factors which are responsible for the U-shaped curves of the bonding energies. The separate presentation of the values of ΔE_{elstat} and ΔE_{orb} makes it also possible to estimate the electrostatic and covalent contributions to the metal–CO bonding interactions.

in the geometry of the complex. ΔE_{Pauli} gives the repulsive interaction energy between the fragments which is caused by the fact that two electrons with the same spin cannot occupy the same region in space. The term comprises the four-electron destabilizing interactions between occupied orbitals. ΔE_{Pauli} is calculated by enforcing the Kohn–Sham determinant of AB, which is the result of superimposing fragments A and B, to obey the Pauli principle through antisymmetrization and renormalization. The stabilizing orbital interaction term ΔE_{orb} is calculated in the final step of the ETS analysis when the Kohn–Sham orbitals relax to their optimal form. The reader should note that the relaxation energy of the Kohn–Sham orbitals includes the effect of electron correlation. The ΔE_{orb} term can be further partitioned into contributions by orbitals which belong to different irreducible representations of the interacting system.

Results and Discussion

The discussion of the results is organized in the following way. First, we summarize the calculated geometries, the bond dissociation energies (BDE), and the atomic partial charges of the hexacarbonyls. This section is rather short because part of the data have been reported before.¹⁶ In the following parts we discuss the results of the bonding analysis. The second section

Table 1. Calculated Bond Dissociation Energies (kcal/mol) and Interatomic Distances (Å) and Atomic Partial Charges (e) According to the Hirshfeld Partitioning Scheme

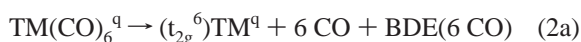
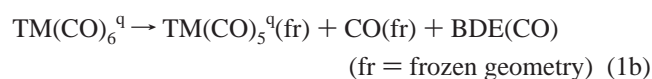
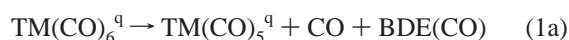
		$\text{Hf}(\text{CO})_6^{2-}$	$\text{Ta}(\text{CO})_6^-$	$\text{W}(\text{CO})_6$	$\text{Re}(\text{CO})_6^+$	$\text{Os}(\text{CO})_6^{2+}$	$\text{Ir}(\text{CO})_6^{3+}$
reaction	no.	bonding energy					
$\text{TM}(\text{CO})_5^q + \text{CO}$	1a	-50.84	-48.26	-45.98	-48.36	-56.92	-73.74
$\text{TM}(\text{CO})_5^q(\text{fr}) + \text{CO}(\text{fr})$	1b	-56.59	-51.31	-49.63	-52.74	-61.92	-78.90
$\text{TM}^q(t_{2g}^6) + 6\text{CO}$	2a	-511.10	-498.24	-448.37	-439.51	-517.25	-774.71
$\text{TM}^q(t_{2g}^6) + (\text{CO})_6(\text{fr})$	2b	-543.90	-525.56	-473.89	-456.57	-544.40	-801.58
bond		distances ^a					
TM-C		2.195 (2.174–2.180)	2.112 (2.083)	2.061 (2.058)	2.036 (1.98–2.07)	2.034	2.055 (2.00–2.05)
C-O		1.185 (1.165)	1.169 (1.149)	1.153 (1.148)	1.139 (1.14–1.19)	1.129	1.129 (1.07–1.12)
atom		Hirshfeld charges					
TM		-0.065	0.016	0.079	0.148	0.226	0.337
C		-0.055	0.017	0.089	0.157	0.222	0.282
O		-0.268	-0.187	-0.102	-0.015	0.074	0.162

^a Experimental values are given in parentheses.^{31,38}

gives an account of the interactions between CO and the metal pentacarbonyl fragments. In the third section we present a bonding analysis of the interactions between the metal atom, TM^q , and the ligand cage, $(\text{CO})_6$. The final section contains an analysis of the contributions of the metal d, s, and p valence orbitals to the carbonyl bonds.

Geometries, Bond Energies, and Charge Distribution.

Table 1 shows two types of calculated bonding energies. First, we give the theoretically predicted bond dissociation energies (BDEs), D_e , of the metal hexacarbonyls for loss of one CO ligand yielding $\text{TM}(\text{CO})_5^q$ and CO in the relaxed geometries (eq 1a) and in the frozen geometries of the hexacarbonyls (eq 1b). The latter set gives the instantaneous interaction energies, ΔE_{int} , between the pentacarbonyl fragment and CO in the complex. The two sets of data from reactions 1a and 1b are not very different, because the geometry changes of the fragments are very small. The D_e value of $\text{W}(\text{CO})_6$ (49.63 kcal/mol) gives a ZPE corrected theoretically predicted BDE of $\text{W}(\text{CO})_6$ $D_0 = 47.5$ kcal/mol which is in excellent agreement with the experimental value $D_0 = 46 \pm 2$ kcal/mol.³⁰ The theoretical D_e and ΔE_{int} values show the same U-shaped trend from $\text{Hf}(\text{CO})_6^{2-}$ to $\text{Ir}(\text{CO})_6^{3+}$ with $\text{W}(\text{CO})_6$ being the lowest point in the curve as found in our previous study.¹⁶



The second set of bonding energies given in Table 1 refers to the dissociation of $\text{TM}(\text{CO})_6^q$ into the metal cation in the t_{2g}^6 reference state, which is the valence state of the metal in the hexacarbonyl, and six CO (eq 2). Equation 2a gives the calculated BDEs for the reactions yielding 6 CO with optimized bond lengths, while eq 2b describes the dissociation yielding the metal and the ligand cage $(\text{CO})_6$ in the frozen geometry of the hexacarbonyl. Both sets of BDEs exhibit a similar U-shaped curve like the BDEs for loss of one CO. However, the lowest

BDEs of eqs 2a and 2b are predicted for $\text{Re}(\text{CO})_6^+$ (Table 1). The highest bonding energies of eqs 1 and 2 are calculated for $\text{Ir}(\text{CO})_6^{3+}$.

Table 1 shows that the calculated metal-CO bond lengths $R(\text{TM}-\text{C})$ are in excellent agreement with experimental values.^{31,38} Please note that the $R(\text{TM}-\text{C})$ values decrease regularly from $\text{Hf}(\text{CO})_6^{2-}$ to $\text{Os}(\text{CO})_6^{2+}$ before they become longer again in triply charged $\text{Ir}(\text{CO})_6^{3+}$. The calculations predict that the C-O bond lengths decrease regularly from $\text{Hf}(\text{CO})_6^{2-}$ to $\text{Ir}(\text{CO})_6^{3+}$. The experimental values for $R(\text{C}-\text{O})$ agree with the theoretical trend, but the scattering of the measured values is rather high. The regular increase of the C-O stretching frequency from $\text{Hf}(\text{CO})_6^{2-}$ to $\text{Ir}(\text{CO})_6^{3+}$ with intervals of ~ 100 cm^{-1} , which was found experimentally³¹ and theoretically,^{16,32} is in agreement with the trend toward shorter C-O interatomic distances.

The charge distribution given by the Hirshfeld partitioning scheme indicates a regular decrease of negative charge (increase of positive charge) for the three atom types, TM, C, O, from $\text{Hf}(\text{CO})_6^{2-}$ to $\text{Ir}(\text{CO})_6^{3+}$. This is a reasonable trend. The previous study of SF gave NBO partial charges, which show larger charge separations and a less regular trend of the charge distribution.¹⁶

Energy Decomposition $\text{TM}^q(\text{CO})_5-\text{CO}$. Table 2 shows the results of the partitioning of the interaction energies, $E_{\text{int}}(\text{CO})$, between $\text{TM}(\text{CO})_5^q$ and CO into the three terms, ΔE_{Pauli} , ΔE_{elstat} , and ΔE_{orb} . The trends of the different energy terms are displayed in Figure 3.

Figure 3 shows that the ΔE_{orb} values indeed have a similar trend as the total interaction energies, ΔE_{int} , but the ΔE_{int} values increase from $\text{W}(\text{CO})_6$ to $\text{Hf}(\text{CO})_6^{2-}$ while the ΔE_{orb} values decrease (Table 2). The similar trends of ΔE_{int} and ΔE_{orb} exhibited in Figure 3 support the idea that the bond strength can be correlated with the orbital interactions, but the opposite behavior of the two terms from $\text{W}(\text{CO})_6$ to $\text{Hf}(\text{CO})_6^{2-}$ demonstrates that other factors can also be important. Figure 3 shows that the sum of ΔE_{Pauli} and ΔE_{orb} gives a trend which is in agreement with the increase of ΔE_{int} , $\text{W}(\text{CO})_6 < \text{Ta}(\text{CO})_6^- <$

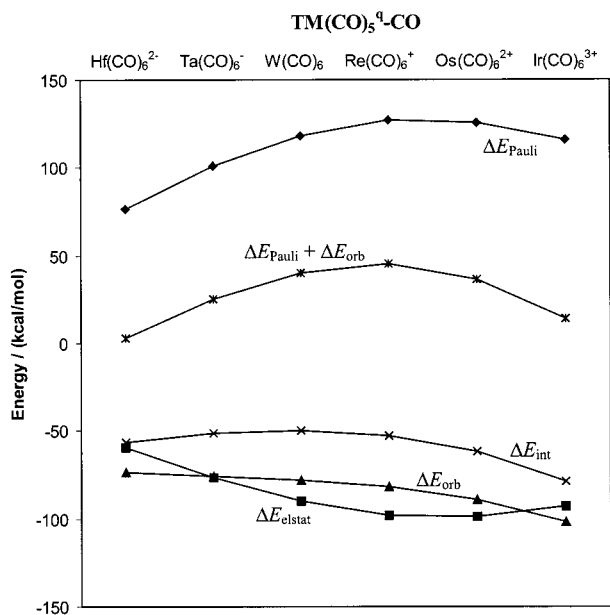
(30) Lewis, K. E.; Golden, D. M.; Smith, G. P. *J. Am. Chem. Soc.* **1984**, *106*, 3905.

(31) (a) Ellis, J. E.; Chi, K.-M. *J. Am. Chem. Soc.* **1990**, *112*, 6022. (b) Siebert, H. *Anwendungen der Schwingungsspektroskopie in der anorganischen Chemie*; Springer: Berlin, Germany, 1966. (c) Jones, L. H.; McDowell, R. S.; Goldblatt, M. *Inorg. Chem.* **1969**, *8*, 2349. (d) Abel, E. W.; McLean, R. A. N.; Tyfield, S. P.; Braterman, P. S.; Walker, A. P.; Hendra, P. J. *J. Mol. Spectrosc.* **1969**, *30*, 29. (e) Wang, C.; Bley, B.; Balzer-Jöllenbeck, G.; Lewis, A. R.; Siu, S. C.; Willner, H.; Aubke, F. *J. Chem. Soc., Chem. Commun.* **1995**, 2071. (f) Bach, C.; Willner, H.; Wang, C.; Rettig, S. J.; Trotter, J.; Aubke, F. *Angew. Chem.* **1996**, *108*, 2104; *Angew. Chem., Int. Ed. Engl.* **1996**, *35*, 1974.

(32) Jonas, V.; Thiel, W. *Organometallics* **1998**, *17*, 353.

Table 2. Energy Decomposition and Bonding Analysis of $\text{TM}(\text{CO})_5^q + \text{CO}$

	$\text{Hf}(\text{CO})_6^{2-}$	$\text{Ta}(\text{CO})_6^-$	$\text{W}(\text{CO})_6$	$\text{Re}(\text{CO})_6^+$	$\text{Os}(\text{CO})_6^{2+}$	$\text{Ir}(\text{CO})_6^{3+}$
	energy decomposition (kcal/mol)					
ΔE_{int}	-56.59	-51.31	-49.63	-52.74	-61.92	-78.90
ΔE_{Pauli}	76.63	100.74	118.31	126.86	125.44	115.94
ΔE_{elstat}	-59.38	-76.56	-90.08	-97.69	-98.48	-93.08
ΔE_{orb}	-73.83	-75.48	-77.87	-81.92	-88.87	-101.76
A_1	-17.19	-25.79	-35.92	-47.34	-60.08	-75.39
A_2	0.00	0.00	0.00	0.00	0.00	0.00
B_1	0.05	0.02	-0.03	-0.07	-0.09	-0.10
B_2	-0.05	-0.07	-0.07	-0.07	-0.06	-0.05
E	-56.64	-49.64	-41.85	-34.44	-28.64	-26.22
	orbital overlap $\langle \text{TM}(\text{CO})_5^q \text{CO} \rangle$					
$\langle 11a_1 5\sigma \rangle$	0.428	0.446	0.468	0.486	0.476	0.414
$\langle 10e 2\pi \rangle$	0.194	0.197	0.192	0.179	0.155	0.108
	orbital population/e					
-- Σ --						
$\text{TM}(\text{CO})_5^q$	$11a_1$	0.18	0.21	0.26	0.34	0.43
CO	5σ	1.72	1.70	1.68	1.64	1.52
-- Π --						
$\text{TM}(\text{CO})_5^q$	$10e$	1.67	1.75	1.81	1.87	1.96
CO	2π	0.35	0.28	0.21	0.15	0.07

**Figure 3.** Trend of the energy contributions to the interaction energy between $\text{TM}^q(\text{CO})_5$ and CO .

$\text{Hf}(\text{CO})_6^{2-}$, but the highest point of the curve is found for $\text{Re}(\text{CO})_6^+$ and not for $\text{W}(\text{CO})_6$.

An important point concerns the absolute values of the energy terms ΔE_{Pauli} , ΔE_{elstat} , and ΔE_{orb} . Table 2 shows that the calculated values of ΔE_{elstat} and ΔE_{orb} are always higher than the bonding energy, ΔE_{int} . An arbitrary consideration of only one attractive term would lead to the conclusion that the CO ligand either is only electrostatically bound or that it is only covalently bound. A reasonable consideration of all three terms leads to the conclusion that the ionic contribution and the covalent contribution to the $(\text{CO})_5\text{TM}^q\text{-CO}$ bonding interactions have a similar size and that the Pauli repulsion leads to a net bonding which is $< 0.5(\Delta E_{\text{elstat}} + \Delta E_{\text{orb}})$. Figure 3 shows that, for $\text{Hf}(\text{CO})_6^{2-}$ and $\text{Ir}(\text{CO})_6^{3+}$, the covalent bonding given by ΔE_{orb} is larger than the electrostatic bonding given by ΔE_{elstat} , while for $\text{W}(\text{CO})_6$, $\text{Re}(\text{CO})_6^+$, and $\text{Os}(\text{CO})_6^{2+}$, it holds that $\Delta E_{\text{orb}} < \Delta E_{\text{elstat}}$. This is a counterintuitive result, because it means that the highest charged complexes have the smallest degree of ionic character in the metal-CO bond.

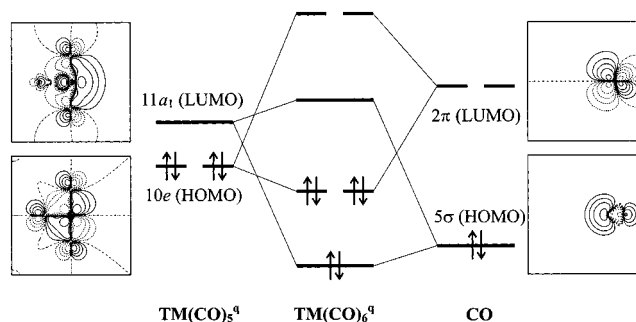
**Figure 4.** Orbital interaction diagram and plot of the HOMO and LUMO of $\text{TM}^q(\text{CO})_5$ and CO .

Table 2 shows that the values for ΔE_{Pauli} and ΔE_{elstat} have a trend which follows the TM-CO bond lengths, i.e., the absolute values increase with the shortening of the bond from $\text{Hf}(\text{CO})_6^{2-}$ to $\text{Os}(\text{CO})_6^{2+}$ but decrease for $\text{Ir}(\text{CO})_6^{3+}$. We want to point out that the ΔE_{elstat} value of $\text{Ir}(\text{CO})_6^{3+}$ is less than those of $\text{Re}(\text{CO})_6^+$ and $\text{Os}(\text{CO})_6^{2+}$. This means that the very high bonding energy of the iridium complex cannot be explained with electrostatic forces.

Table 2 also gives the contributions of the stabilizing orbital interaction term, ΔE_{orb} , for the orbitals with different symmetry. Figure 4 shows a contour-line diagram of the symmetry-allowed orbital interactions between the HOMO and LUMO of the fragments which can be expected to give the largest contributions to the ΔE_{orb} term. Table 2 shows that only the orbital interactions with a_1 and e symmetry significantly contribute to the ΔE_{orb} term. Although the stabilization arises from the sum of all orbital interactions with a_1 and e symmetry, it can reasonably be argued that the dominant contributions come from the HOMO/LUMO interactions depicted in Figure 4. This is supported by the calculated orbital population given in Table 2, which shows that the HOMO and the LUMO exhibit a large change in the population along the series of molecules. It follows that the stabilizing orbital interactions are mainly given by $\text{TM}^q\text{-CO}$ σ -donation (a_1 term) and the $\text{TM}^q\text{-CO}$ π -back-donation (e term).

We want to comment on the trend of the energies given by the a_1 and e symmetric orbital interactions. Table 2 shows that the stabilization due to $\text{TM}^q\text{-CO}$ σ -donation steadily increases from $\text{Hf}(\text{CO})_6^{2-}$ to $\text{Ir}(\text{CO})_6^{3+}$, while the $\text{TM}^q\text{-CO}$ π -back-

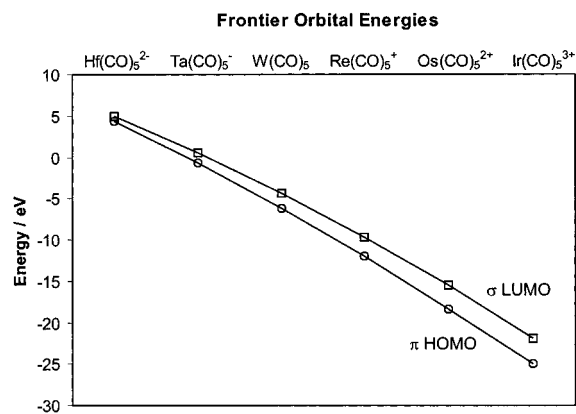


Figure 5. Trend of the frontier orbital energy levels of the pentacarbonyls.

donation exhibits the opposite trend. The stabilization due to π -back-donation in $\text{Hf}(\text{CO})_6^{2-}$, $\text{Ta}(\text{CO})_6^-$, and $\text{W}(\text{CO})_6$ is stronger than the σ -donation, while the positively charged hexacarbonyls have stronger σ -donation than π -back-donation. The trends can be explained with the lowering of the orbital energies of the $10e$ HOMO and $11a_1$ LUMO of $\text{TM}(\text{CO})_5^q$ from $\text{Hf}(\text{CO})_6^{2-}$ to $\text{Ir}(\text{CO})_6^{3+}$. Figure 5 shows that the energy levels of the frontier orbitals of $\text{TM}(\text{CO})_5^q$ span a wide range from +5 to -25 eV. The very low lying σ LUMO of $\text{Ir}(\text{CO})_5^{3+}$ and the very high lying π HOMO of $\text{Hf}(\text{CO})_5^{2-}$ explain why the $\text{TM}^q \leftarrow \text{CO}$ σ -donation in the iridium complex and the $\text{TM}^q \rightarrow \text{CO}$ π -back-donation in the hafnium complex dominate the stabilizing orbital interactions in the compounds (Table 2). Table 2 shows also that the orbital overlap between the 5σ HOMO of CO and $11a_1$ LUMO of $\text{TM}(\text{CO})_5^q$ does not change very much for the six interacting systems. Nor does the overlap between the $10e$ HOMO of $\text{TM}(\text{CO})_5^q$ and the 2π LUMO of CO vary noticeably among the first four species listed in Table 2. Please note that $\text{Ir}(\text{CO})_6^{3+}$, which has the strongest contribution by (a_1) σ -donation, has the smallest orbital overlap $\langle 11a_1/5\sigma \rangle$. It follows that orbital overlap is here overruled by the factor of matching orbital energies.

The calculated orbital population shows a steady increase of the $11a_1$ LUMO of the metal fragment and a decrease of the 2π LUMO population of CO from $\text{Hf}(\text{CO})_6^{2-}$ to $\text{Ir}(\text{CO})_6^{3+}$. The same trends have been found by SF in the CDA analysis of the compounds.¹⁶ The change in the orbital population agrees with the trend of the orbital interaction energies. The values in Table 2 demonstrate that the size of the orbital overlap between the bonded atoms does not correlate with the bond energy. The overlap of the σ orbital $\langle 11a_1/5\sigma \rangle$ in $\text{Hf}(\text{CO})_6^{2-}$, $\text{Ta}(\text{CO})_6^-$, and $\text{W}(\text{CO})_6$ is larger than the overlap of the π orbital $\langle 11e/2\pi \rangle$ and yet, the π -bonding energy is higher than the σ -bonding energy. Also, the trend of the orbital overlaps and the associated energy values do not agree with each other. The σ orbital overlap $\langle 11a_1/5\sigma \rangle$ of $\text{Ir}(\text{CO})_6^{3+}$ has the smallest value (0.414) of the carbonyl complexes, but the energy contribution is the largest of all compounds (Table 2). The change in the orbital overlap population of the σ and π orbitals, however, agrees with the relative contributions of the associated energies to ΔE_{orb} . The π -orbital populations of $\text{Hf}(\text{CO})_6^{2-}$, $\text{Ta}(\text{CO})_6^-$, and $\text{W}(\text{CO})_6$ are larger than the σ population, while the opposite is found for the cations. Note that the values for the orbital overlap and for the orbital contribution given in Table 2 refer to only one component of the degenerate π orbital. They must be multiplied by two in order to get the total values.

Now we try to rationalize the U-shaped trend of the bonding energy, ΔE_{int} , in light of the calculated values for the various

terms of the ETS analysis. We use the results for $\text{W}(\text{CO})_6$, which has the lowest E_{int} value and the lowest BDE, as a reference point. It becomes obvious that the higher $\text{TM}(\text{CO})_5^q \leftarrow \text{CO}$ interaction energies of the negatively charged complexes $\text{Ta}(\text{CO})_6^-$ and $\text{Hf}(\text{CO})_6^{2-}$ are *not* caused by the changes in the electrostatic attraction, which decreases for the anions, nor by the ΔE_{orb} term, which also becomes slightly smaller. The higher bonding energy is rather caused by the very large decrease in the repulsive, ΔE_{Pauli} , term (Table 2). Although the stabilizing $\text{TM}(\text{CO})_5^q \rightarrow \text{CO}$ π -back-donation becomes larger in the anions, the increase is compensated for by the larger decrease in the $\text{TM}(\text{CO})_5^q \leftarrow \text{CO}$ σ -donation. The overall stabilization by the ΔE_{orb} term in $\text{Ta}(\text{CO})_6^-$ and $\text{Hf}(\text{CO})_6^{2-}$ is weaker than that in $\text{W}(\text{CO})_6$. A superficial consideration of the trend of the different terms could have attributed the higher BDEs of the anions to the increase in the π -back-donation.

A different explanation must be given for the higher bond energies of the positively charged systems. Table 2 shows that the increase of the ΔE_{int} values from $\text{W}(\text{CO})_6$ to $\text{Ir}(\text{CO})_6^{3+}$ runs parallel to the increase of the ΔE_{orb} values. This is because the sum of the Pauli repulsion and electrostatic attraction is nearly constant for $\text{W}(\text{CO})_6$, $\text{Re}(\text{CO})_6^+$, and $\text{Os}(\text{CO})_6^{2+}$ (Figure 3). Thus, it seems reasonable to conclude that the larger E_{int} values of $\text{Re}(\text{CO})_6^+$, $\text{Os}(\text{CO})_6^{2+}$, and $\text{Ir}(\text{CO})_6^{3+}$ are caused by the larger ΔE_{orb} values, which come from the stronger $\text{TM}(\text{CO})_5^q \leftarrow \text{CO}$ σ -donation. However, the electrostatic attraction also increases from $\text{W}(\text{CO})_6$ to $\text{Os}(\text{CO})_6^{2+}$, and the further increase of the ΔE_{int} value for $\text{Ir}(\text{CO})_6^{3+}$ may also be explained with the decrease of Pauli repulsion. It is arbitrary to state that the higher interaction energies are *caused* by the ΔE_{orb} term. All one can say is that the increase of the ΔE_{int} values from $\text{W}(\text{CO})_6$ to $\text{Ir}(\text{CO})_6^{3+}$ can be *correlated* with the increase of the ΔE_{orb} term.

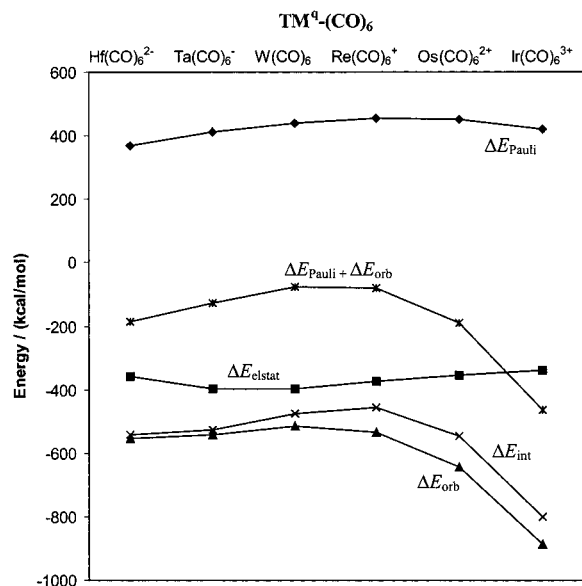
Energy Decomposition $\text{TM}^q \leftarrow (\text{CO})_6$. Table 3 gives the energy contributions ΔE_{Pauli} , ΔE_{elstat} , and ΔE_{orb} to the total interaction energy, ΔE_{int} , between the metal, TM^q , and the ligand cage, $(\text{CO})_6$. Figure 6 shows the trend of the energy terms from $\text{Hf}(\text{CO})_6^{2-}$ to $\text{Ir}(\text{CO})_6^{3+}$. It becomes obvious that the values of the orbital interaction term, ΔE_{orb} , are quite similar to the ΔE_{int} values and that the two curves exhibit a similar shape. The only qualitative difference between the two terms is found for $\text{W}(\text{CO})_6$ and $\text{Re}(\text{CO})_6^+$. The total interaction energy decreases from $\text{W}(\text{CO})_6$ to $\text{Re}(\text{CO})_6^+$, while the orbital interactions increase in this direction (Table 3). A similar trend as for ΔE_{orb} is found for the total orbital interactions, $\Delta E_{\text{orb}} + \Delta E_{\text{Pauli}}$ (Figure 6). This is because the values of the Pauli repulsion and the electrostatic interactions, ΔE_{elstat} , change only little from $\text{Hf}(\text{CO})_6^{2-}$ to $\text{Ir}(\text{CO})_6^{3+}$, although the charge of the complexes varies from -2 to +3. We want to point out that the electrostatic attraction between Ir^{3+} and $(\text{CO})_6$ is the smallest of that of the hexacarbonyls shown in Table 3, although the metal carries the largest charge and $\text{Ir}(\text{CO})_6^{3+}$ has the largest $\text{TM}^q \leftarrow (\text{CO})_6$ interaction energy. Thus, the electrostatic interactions are not the reason for the large bonding energy in $\text{Ir}(\text{CO})_6^{3+}$ and they do not play a role for the trend of the metal-CO interactions. Note that the trend of the ΔE_{elstat} values given in Table 3 does not follow the pattern of the metal-CO distances, unlike the values which were calculated for the interactions between $\text{TM}(\text{CO})_5^q$ and CO (Table 2).

The energy decomposition of the total binding energy of the hexacarbonyls $\text{TM}(\text{CO})_6^q$ in terms of interactions between TM^q and $(\text{CO})_6$ in the geometry of the complex retains O_h symmetry. This makes it possible to analyze the different orbital interactions of the metal valence orbitals having different symmetry and to estimate their contributions to the σ - and π -type interactions

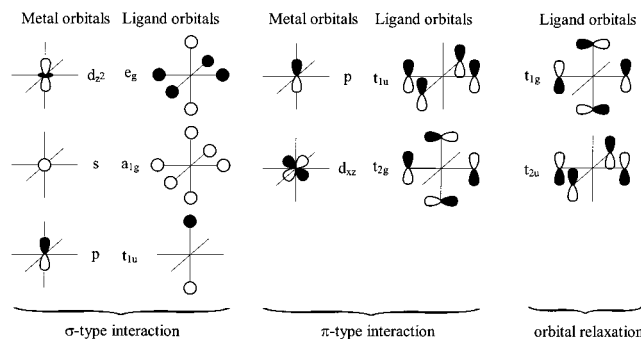
Table 3. Energy Decomposition and Bonding Analysis of $\text{TM}^q + (\text{CO})_6$

	$\text{Hf}(\text{CO})_6^{2-}$	$\text{Ta}(\text{CO})_6^-$	$\text{W}(\text{CO})_6$	$\text{Re}(\text{CO})_6^+$	$\text{Os}(\text{CO})_6^{2+}$	$\text{Ir}(\text{CO})_6^{3+}$	
energy decomposition (kcal/mol)							
ΔE_{int}	-543.90	-525.56	-473.89	-456.57	-544.40	-801.58	
ΔE_{Pauli}	367.40	413.38	438.80	454.51	451.33	420.93	
ΔE_{elstat}	-358.62	-397.62	-396.24	-375.09	-353.44	-337.81	
ΔE_{orb}	-552.68	-541.32	-516.44	-536.00	-642.27	-884.70	
A_{1g}	-9.48	-10.49	-15.40	-27.42	-47.63	-78.78	
A_{2g}	0.00	0.00	0.00	0.00	0.00	0.00	
E_g	-83.36	-113.07	-159.08	-233.72	-348.84	-520.66	
T_{1g}	-1.30	-0.98	-2.88	-8.91	-19.41	-33.92	
T_{2g}	-437.42	-397.59	-308.18	-200.33	-101.14	-43.82	
A_{1u}	-0.03	-0.04	-0.03	0.00	-0.02	-0.02	
E_u	0.00	-0.00	0.00	0.00	0.00	0.00	
T_{2u}	-2.74	-2.00	-4.35	-11.60	-23.86	-40.17	
T_{1u}	-18.35	-17.15	-26.52	-54.00	-101.37	-167.33	
$T_{1u}(\sigma)^a$	-12.97	-12.06	-18.65	-38.53	-73.98	-125.68	
$T_{1u}(\pi)^b$	-5.38	-5.09	-7.87	-15.47	-27.39	-41.65	
orbital overlap $\langle \text{TM}^q (\text{CO})_6 \rangle$							
$\langle 2a_{1g} 3a_{1g} \rangle$	0.656	0.683	0.708	0.713	0.697	0.659	
$\langle 1e_g 3e_g \rangle$	0.620	0.619	0.573	0.495	0.412	0.329	
$\langle 1t_{2g} 2t_{2g} \rangle$	0.524	0.505	0.440	0.345	0.273	0.204	
$\langle 3t_{1u} 3t_{1u} \rangle$	0.261	0.274	0.281	0.275	0.257	0.226	
$\langle 3t_{1u} 4t_{1u} \rangle$	0.629	0.649	0.666	0.685	0.694	0.682	
orbital population/e							
-- A_{1g} --							
TM^q	$2a_{1g}$	0.16	0.19	0.24	0.33	0.41	0.50
$(\text{CO})_6$	$3a_{1g}$	1.76	1.76	1.76	1.72	1.66	1.56
-- E_g --							
TM^q	$1e_g$	0.41	0.55	0.66	0.73	0.83	0.91
$(\text{CO})_6$	$3e_g$	1.55	1.46	1.37	1.28	1.18	1.05
-- T_{2g} --							
TM^q	$1t_{2g}$	0.60	0.99	1.29	1.46	1.61	1.75
$(\text{CO})_6$	$2t_{2g}$	1.36	1.03	0.74	0.52	0.34	0.19
-- T_{1u} --							
TM^q	$3t_{1u}$	0.07	0.07	0.09	0.12	0.15	0.20
$(\text{CO})_6$	$3t_{1u}$	1.97	1.96	1.95	1.94	1.93	1.93
$(\text{CO})_6$	$4t_{1u}$	1.93	1.95	1.95	1.93	1.90	1.84

^a $E(\text{T}_{1u})(\sigma) = E(\text{T}_{1u}) \cdot \langle 3t_{1u} | 4t_{1u} \rangle / (\langle 3t_{1u} | 3t_{1u} \rangle + \langle 3t_{1u} | 4t_{1u} \rangle)$. ^b $E(\text{T}_{1u})(\pi) = E(\text{T}_{1u}) \cdot \langle 3t_{1u} | 3t_{1u} \rangle / (\langle 3t_{1u} | 3t_{1u} \rangle + \langle 3t_{1u} | 4t_{1u} \rangle)$.

**Figure 6.** Trend of the energy contributions to the interaction energy between TM^q and $(\text{CO})_6$.

with the ligand-cage orbitals. Figure 2 suggests that σ interactions arise from orbitals with t_{1u} , e_g , and a_{1g} symmetry, while the π interactions come from orbitals which have t_{2g} symmetry. Table 2 shows that the partitioning of the ΔE_{orb} term gives also contributions from orbitals which have t_{1g} and t_{2u} symmetry. Figure 7 shows a more detailed representation of the orbital interactions $\text{TM}^q-(\text{CO})_6$ as given in Figure 2.

**Figure 7.** Schematic representation of the orbitals with different symmetry which contribute to the ΔE_{orb} term according to the ETS analysis of $\text{TM}^q-(\text{CO})_6$ (Table 3).

It becomes obvious that the metal valence orbitals which are engaged in σ -type interactions with $(\text{CO})_6$ are the d_{z^2} and (not shown in Figure 7) the $d_{x^2-y^2}$ orbitals (e.g., symmetry), the s orbital (a_{1g}), and the p orbitals (t_{1u}). The π -type interactions involve the d_{xz} and (not shown) d_{xy} and d_{yz} orbitals (t_{2g}), but also the p orbitals of the metal which can form a t_{1u} combination with the π orbitals of $(\text{CO})_6$. The latter stands for the donation of the occupied π MOs of CO into empty $p(\pi)$ AOs of the metal. The contribution of this interaction to the metal-CO π -bonding is not shown in Figure 2. It is often neglected, but a popular textbook of organometallic chemistry has pointed out that TM^q-CO π -donation may perhaps also be important.³³ Thus,

(33) Elschenbroich, Ch.; Salzer, A. *Organometallics*, 2nd ed.; VCH: Weinheim, Germany, 1992.

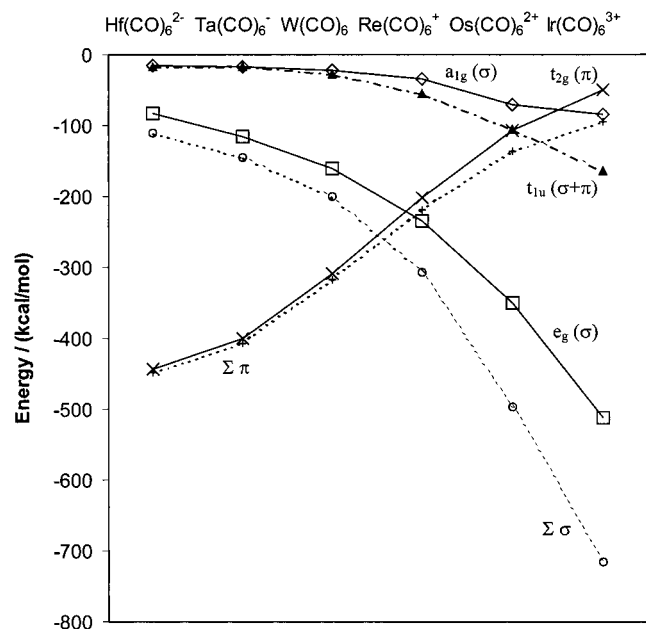


Figure 8. Trend of the contributions of the orbital interaction term ΔE_{orb} to the binding energy of $\text{TM}^q-(\text{CO})_6$.

the total t_{1u} contribution of the orbital interaction term, ΔE_{orb} , gives not only the stabilization due to $\text{TM}-\text{CO}$ σ -donation but it contains also the stabilization due to $\text{TM}-\text{CO}$ π -donation. To quantify the σ and π contributions to the t_{1u} symmetric ΔE_{orb} term, we used as a rough approximation the size of the overlaps of the metal p orbital with the $3t_{1u}$ and $4t_{1u}$ orbitals of $(\text{CO})_6$, which consist primarily of π and σ CO orbitals, respectively.³⁴ Table 3 shows that the energy contribution of the $\text{TM}-\text{CO}$ π -donation is always much less than the $\text{TM}-\text{CO}$ σ -donation. We want to point out that the division of the t_{1u} orbital interactions into σ and π contributions is not very relevant to the other conclusions which are made in this paper.

The remaining contributions to the ΔE_{orb} term have t_{1g} and t_{2u} symmetry (Figure 7). The t_{1g} and t_{2u} contributions are not genuine orbital interaction terms. There are no metal orbitals which have t_{1g} or t_{2u} symmetry in an octahedral environment. The stabilization arises from the relaxation of the occupied t_{1g} and t_{2u} ligand orbitals of $(\text{CO})_6$ caused by the electrostatic attraction of the metal. The electric charge of the metal polarizes the electronic charge distribution of the carbonyl ligands. It has been shown by us³⁵ and by others³⁶ that the charge distribution of CO, which is caused by a positive point charge, has a strong effect on the C–O bond length and stretching frequency. The electrostatic stabilization of the t_{1g} and t_{2u} ligand orbitals is quite small in the neutral and negatively charged carbonyls, but it becomes larger in the positively charged species. The size of the t_{1g} and t_{2u} terms in $\text{Ir}(\text{CO})_6^{3+}$ eventually becomes comparable to the (t_{2g}) $\text{Ir}^{3+} \rightarrow (\text{CO})_6$ π -back-donation (Table 3).

Figure 8 shows graphically the trend of the σ and π orbital interaction energies with different symmetries which contribute to the $\text{TM}^q-(\text{CO})_6$ donation (e_g , a_{1g} , t_{1u}) and the $\text{TM}^q \rightarrow (\text{CO})_6$

back-donation (t_{2g}). Note that the total π interaction includes the t_{1u} $\text{TM}^q \leftarrow (\text{CO})_6$ π -back-donation. It becomes obvious that, for the negatively charged and neutral species, the π interactions are more important than the σ interactions, while the σ interactions dominate the ΔE_{orb} term for the positively charged metal carbonyls. The largest part of the π interactions comes from the t_{2g} term, while the largest contribution to the σ interactions comes from the e_g orbital.

We also analyzed the changes in the electronic structure of the metal and the ligand cage by the bonding interactions. Table 3 shows that the calculated orbital overlaps $\langle \text{TM}^q/(\text{CO})_6 \rangle$ again do not correlate at all with the energy contributions. Thus, in the systems investigated here, the energy difference between the occupied and empty orbitals is much more important for the ΔE_{orb} value than the orbital overlap.

Valence Orbitals of the Transition Metals. Figure 7 shows that the empty d(σ), s, and p valence orbitals of the metal receive electronic charge from the $(\text{CO})_6$ ligand through orbitals having e_g , a_{1g} , and t_{1u} symmetry. The respective energy terms may thus be used to estimate how important the metal orbitals are for the strength of the metal–ligand interactions.³⁷ The values given in Table 3 show for all metals the order $e_g \gg t_{1u} > a_{1g}$. To relate this to the metal valence orbitals, the degeneracy of the orbitals must be considered. There are two d orbitals, one s orbital, and three p orbitals of the metal involved. This leads to the energy contributions by a single d, s, or p metal orbital which are shown in Table 4. It becomes obvious that the relative importance of the TM valence orbitals is $d \gg s > p$. The size of a single p orbital contribution to the ΔE_{orb} energy term is between 54 and 71% of the s orbital contribution. The metal d valence orbital is much more important energywise than the s and p orbitals. However, the *total* contribution of the three p orbitals is larger than the contribution of the s orbital.

The valence orbital populations which are also shown in Table 3 indicate the charge exchange between the metal and the ligand cage. The orbital populations correlate nicely with the trend of the orbital interaction energies, similar to that which was found before for the $(\text{CO})_5\text{TM}^q-\text{CO}$ systems. Table 4 also gives the contributions of the d(σ), s, and p valence orbitals of the metals to the total $\text{TM}^q-(\text{CO})_6$ charge acceptance. The $2a_{1g}$ acceptor orbital of Hf^{2-} , which is the empty valence s orbital in the t_{2g}^6 state, receives only 0.16 electrons from $(\text{CO})_6$ in $\text{Hf}(\text{CO})_6^{2-}$, while 0.50 electrons are donated into the valence s orbital of Ir^{3+} . The $\text{TM}^q \leftarrow (\text{CO})_6$ σ -donation into the d(σ) orbitals of TM^q is significantly higher. The e_g donation in $\text{Hf}(\text{CO})_6^{2-}$ is 0.41 electrons, and it increases to 0.91 electrons in $\text{Ir}(\text{CO})_6^{3+}$. Significantly smaller charge donations are found for the ligand donation into the metal p orbitals. The (t_{1u}) p orbital population of TM^q is between 0.07 electrons in $\text{Hf}(\text{CO})_6^{2-}$ and 0.20 electrons in $\text{Ir}(\text{CO})_6^{3+}$. However, these are the values for a single p orbital. The total $\text{TM}^q(\text{p}) \leftarrow (\text{CO})_6$ donation into the three metal p orbitals is always larger than the $\text{TM}^q(\text{s}) \leftarrow (\text{CO})_6$ donation. Thus, the breakdown of the charge and energy contributions of the d, s, p metal orbitals in $\text{TM}(\text{CO})_6^q$ suggests that the p orbitals are as important as the s orbital and, therefore, should be considered as true valence orbitals.

(37) Please note that the orbital relaxation step gives the contributions by all s and p orbitals of the metal and not only the valence orbitals. However, the dominant contributions should come from the valence orbitals.

(38) (a) Arnesen, S. V.; Seip, H. M. *Acta Chem. Scand.* **1966**, *20*, 2711. (b) Calderazzo, F.; Englert, U.; Pampaloni, G.; Pelizzi, G.; Zamboni, R. *Inorg. Chem.* **1983**, *22*, 1865. (c) Bruce, D. M.; Holloway, J. H.; Russel, D. R. *J. Chem. Soc., Dalton Trans.* **1978**, 1627. (d) Holloway, J. H.; Senior, J. B.; Szary, A. C. *J. Chem. Soc., Dalton Trans.* **1987**, 741.

(34) We think that the approximation is justified, because we make a comparison within one system and for orbitals which have the same symmetry. The approximation yields an estimate of the π contribution via t_{1u} donation which is probably too high, because the $3t_{1u}(\pi)$ orbital is lower in energy (−11.684 eV) than the $4t_{1u}(\sigma)$ orbital of $(\text{CO})_6$ (−9.060 eV). Thus, the calculated data can be considered as an upper bound for the $\text{TM}-\text{CO}$ π -donation.

(35) Lupinetti, A. J.; Fau, S.; Frenking, G.; Strauss, S. H. *J. Phys. Chem. A* **1997**, *101*, 9551.

(36) Goldman, A. S.; Krogh-Jespersen, K. *J. Am. Chem. Soc.* **1996**, *118*, 12159.

Table 4. Energy and Charge Contributions of a Single TM d, s, p Orbital to the OC \rightarrow TM^q Donation^a

		Hf(CO) ₆ ²⁻	Ta(CO) ₆ ⁻	W(CO) ₆	Re(CO) ₆ ⁺	Os(CO) ₆ ²⁺	Ir(CO) ₆ ³⁺
energy	d	-41.7	-56.5	-79.5	-116.9	-174.4	-260.3
energy	s	-9.5	-10.5	-15.4	-27.4	-47.6	-78.8
energy	p	-6.1	-5.7	-8.8	-18.0	-33.8	-55.8
charge	d	0.41	0.55	0.66	0.73	0.83	0.91
charge	s	0.16	0.19	0.24	0.33	0.41	0.50
charge	p	0.07	0.07	0.09	0.12	0.15	0.20

^a Energy values in kilocalories per mole, charge values in *e*.

Summary

The results of this work can be summarized as follows. The trend of the bond dissociation energies of TM(CO)₆^q for loss of one CO follows a U-shaped curve from Hf(CO)₆²⁻ to Ir(CO)₆³⁺. The lowest BDE is calculated for W(CO)₆. The higher bond dissociation energies of the negatively charged hexacarbonyls Hf(CO)₆²⁻ and Ta(CO)₆⁻ compared with W(CO)₆ are caused by less Pauli repulsion and not by attractive orbital interactions. The increase of the (CO)₅TM^q-CO BDEs of the positively charged hexacarbonyls can be correlated with the stronger orbital interactions due to TM^q \leftarrow CO σ -donation. There is a continuous decrease of the strength of the (CO)₅TM^q \rightarrow CO π -back-donation and increase of the (CO)₅TM^q \leftarrow CO σ -donation from Hf(CO)₆²⁻ to Ir(CO)₆³⁺. The latter interaction dominates the orbital interaction term in the carbonyl cations. Electrostatic attraction and stabilizing orbital interaction have a similar strength in the (CO)₅TM^q-CO bonds. The calculated bond dissociation energies of TM(CO)₆^q yielding TM^q in the *t*_{2g}⁶ valence state and 6 CO also exhibit a U-shaped curve with Re(CO)₆⁺ having the lowest BDE. The trend correlates with the calculated orbital interaction term ΔE_{orb} . Orbital interactions make the largest contributions to the bonding in the highly charged complex Ir(CO)₆³⁺. This holds for the interactions between TM^q and (CO)₆ as well as for (CO)₅TM^q-CO. The breakdown of the ΔE_{orb} term into contributions by orbitals having different symmetry shows that the TM^q \rightarrow (CO)₆ π -dona-

tion is the most important contributor in Hf(CO)₆²⁻, Ta(CO)₆⁻, and W(CO)₆, while TM^q \leftarrow (CO)₆ σ -donation dominates the orbital interaction term in Re(CO)₆⁺, Os(CO)₆²⁺, and Ir(CO)₆³⁺. The contribution of the three metal p orbitals to the energy terms and to the charge terms is slightly higher than the contribution of the s orbital. The metal p orbitals should thus be considered as valence orbitals for describing the bonding in the metal hexacarbonyls.

Acknowledgment. This work was financially supported by the Deutsche Forschungsgemeinschaft (SFB 260 and Graduiertenkolleg Metallorganische Chemie) and by the Fonds der Chemischen Industrie. F.M.B. thanks the DFG for a Habilitation fellowship. A.D. thanks the Fonds der Chemischen Industrie for a doctoral stipendium. Excellent service by the Hochschulrechenzentrum of the Philipps-Universität Marburg is gratefully acknowledged. Additional computer time was provided by the HLRS Stuttgart, HHLRZ Darmstadt, and HRZ Frankfurt.

Supporting Information Available: The cartesian coordinates of the optimized hexacarbonyls, pentacarbonyls, and CO are given. We also give the calculated energies of the optimized compounds. This material is available free of charge via the Internet at <http://pubs.acs.org>.

JA000663G